Materials Characterization and Transmission Analysis in Erbium-doped Gallium Nitride Microresonator Structures

by

David M. Gibbons

Submitted to the Department of Materials Science and Engineering in Partial Fulfillment of the Requirements for the Degree of

Bachelor of Science

at the

Massachusetts Institute of Technology

June 2001

Signature of Author: Signature redacted
Department of Materials Science and Engineering
May 18, 2001

Certified by: Signature redacted
Kazumi Wada
Senior Visiting Lecturer
Thesis Supervisor

Certified by: Signature redacted
Lionel C. Kimerling
Thomas Lord Professor of Materials Science and Engineering
Thesis Supervisor

Accepted by: Signature redacted
Ronald M. Latanision
Chairman, Undergraduate Thesis Committee

Materials Characterization and Transmission Analysis in Erbium-doped Gallium Nitride Microresonator Structures

by

David M. Gibbons

Submitted to the Department of Materials Science and Engineering on May 18, 2001 in Partial Fulfillment of the Requirements for the Degree of Bachelor of Science

ABSTRACT

GaN:Er is an attractive material for room temperature 1.54 μm luminescence enhancement devices for use in telecommunications because it does not experience thermal quenching at room temperature like Si:Er and can be electronically pumped. GaN:Er layers grown by molecular beam epitaxy (MBE) on single crystal substrates have shown excellent room temperature 1.54 μm luminescence, but to integrate GaN:Er into microresonator devices it is necessary to grow a good quality GaN:Er film on an amorphous substrate. This thesis examines the optical properties and morphology of GaN:Er layers grown on Si_3N_4 and SiO_2 substrates, and evaluates two microresonator devices with incorporated GaN:Er layers.

GaN:Er layers grown by MBE on SiO_2 and Si_3N_4 substrates were shown to give room temperature luminescence comparable to that of GaN:Er grown on (111)Si. GaN:Er layers grown on a buffered oxide etched Si_3N_4 substrate showed the best luminescence. The ability to grow good quality layers on amorphous substrates allows GaN:Er to be used in waveguide devices, the first of which studied was the microring resonator. Microring resonators were made by depositing a blanket GaN:Er layer on patterned Si_3N_4 microring structures. These structures were damaged, and transmission measurements were not possible. When looking at surface roughness measurements it appears that channel waveguide structures are unsuitable for GaN:Er grown on amorphous substrates, and so a ridge waveguide structure is proposed to lower this surface roughness scattering loss.

A microcavity with a GaN:Er defect layer and a-Si/a-SiO_2 stacks was fabricated and tested for luminescence enhancement. The refractive index of GaN:Er was determined by reflectance measurements to be 2.1. The layer was not of uniform thickness which led to a broad resonance peak, but a distortion of the spectrum including a lower luminescence at the 1517 nm peak and a higher luminescence at the 1557 nm peak were observed, which suggests enhancement by the microcavity.

Thesis Supervisor: Kazumi Wada
Title: Visiting Senior Lecturer

Acknowledgements

This thesis project has been an incredible learning process, with many successes and frustrations that I could not have completed without the help of many people. I would like to thank Dr. Wada for his guidance and for sharing his knowledge. I also would like to thank Prof. Steckl at the University of Cincinnati for his collaboration on growing such excellent quality GaN:Er layers, without which this thesis would not exist. To many others I also must give thanks. To Sajan Saini, who spent many hours in lab with me on PL and Apollo; offering words of encouragment along the way. To Anu Agarwal and Joe Walsh, who helped me greatly at MTL. To Jurgen Michel for assistance with CL, and Libby Shaw for AFM assistance. To Kevin Chen who provided the PBG stacks for the microcavity, and Desmond Lim who provided the microring structures. To Kevin Lee for help with measurements, Xiaoman Duan for the excellent TEM images, and Yasha Yi for the reflectance measurements on the cavity. Without the tremendous help I received from each of these people this would be a much poorer thesis. And lastly, to Prof. Kimerling, who has assembled a terrific research group of postdocs and graduate students who are always willing to lend a helping hand.

Contents

List of Figures

List of Tables

Chapter 1

Introduction

The optical properties of rare-earth elements such as Erbium (Er) have led to many important photonics applications, including solid-state lasers, components for telecommunications, optical storage devices, and displays. Light emission in these structures is in the visible and the infrared, including the wavelength that minimizes loss in silica-based glass fibers used in telecommunications: 1.54 μm. Microresonator structures have been shown to enhance luminescence of this 1.54 μm light[1] and can be used as optical amplifiers. Early research completed on these structures involves Er-doped Si, which has a low Er solubility and also experiences significant loss in luminescence efficiency at room temperature due to thermal quenching.[2]

1.1 Motivation for GaN:Er

Thermal quenching has been shown to decrease with an increase in bandgap energy[3] and so it is natural to look for wide bandgap materials as host materials for Er. Insulating materials have large bandgaps, and the recent success of the erbium-doped fiber amplifiers (EDFAs) that show excellent gain in the 1.53-1.56 μm window[4] proves that room temperature use of devices employing Er-doped materials is possible. However, an insulator-based system cannot be pumped electronically, and also precludes the

integration of microelectronic and microphotonic systems. A wide bandgap semiconductor is needed.

In determining which wide bandgap semiconductors are useful it is important to consider both Er solubility and processing constraints. High solubility of Er with O in host materials is important because it is these Er atoms that emit light at 1.54 μm. GaN epitaxial layers unintentionally contain 10^{20} O atoms/cm^3, and O co-doping has been shown to enhance Er luminescence.[1] A III-V semiconductor is preferred to a II-VI semiconductor because the trivalent Er atom can most easily substitute into a group III position in the lattice. GaN is a III-V direct gap, wide bandgap semiconductor whose fabrication is understood and is the material used in green and blue emitting diodes and lasers. For these reasons GaN is a promising Er host for use in microphotonics.

1.2 Scope and Objectives

High quality GaN can be grown on dissimilar substrates such as crystalline Si and sapphire.[5] However, Si has a higher refractive index than that of GaN and is not good for cladding. SiO_2 and Si_3N_4, typical cladding materials for waveguides, are amorphous and not appropriate as substrates for high quality epitaxial growth. The challenge is to obtain high quality GaN on a low-index cladding layer.

This thesis is the first examination of emissive GaN:Er layers grown on amorphous substrates. Two types of microresonator devices utilizing GaN:Er, the microring resonator and microcavity resonator, are studied to examine room temperature Er luminescence enhancement. Lastly, suggestions are made for improvement of these devices.

Chapter 2

GaN:Er Films Grown by Molecular Beam Epitaxy on Amorphous Substrates

2.1 Background

2.1.1 Radiative Erbium Emission Mechanisms

Erbium ($^{68}Er_{167}$) is a rare earth element with electronic structure [Xe]$6s^2 4f^{12}$. The unfilled $4f$ shell is responsible for light emission as electrons relax from excited $4f$ states and emit photons of various wavelengths. The unfilled $4f$ shell is screened by the full $5s$ and $5p$ shells so Er has very similar optical properties in different host materials.[2] Normally, transitions within the $4f$ shell are forbidden by quantum mechanical selection rules. However, the microenvironment of a particular Er site causes crystal field splitting among the $4f$ levels, thereby permitting the narrow transition that leads to $\lambda = 1.54$ μm photon emission.[1] Er atoms in such a microenvironment which allows photon emission are termed "optically active." The Er $4f$ energy levels up to the GaN bandgap are shown in figure 2-1.[6] The energies of two common pump laser photons are also shown: Ar (488 nm) and HeCd (325 nm). Photons from an Ar laser have a lower energy than the GaN bandgap, and so they provide intra-center excitation to the Er atoms. Photons from a HeCd laser have a higher energy than the GaN band gap and are absorbed by GaN in the creation of an electron-hole pair that subsequently transfers its energy to the Er atoms.

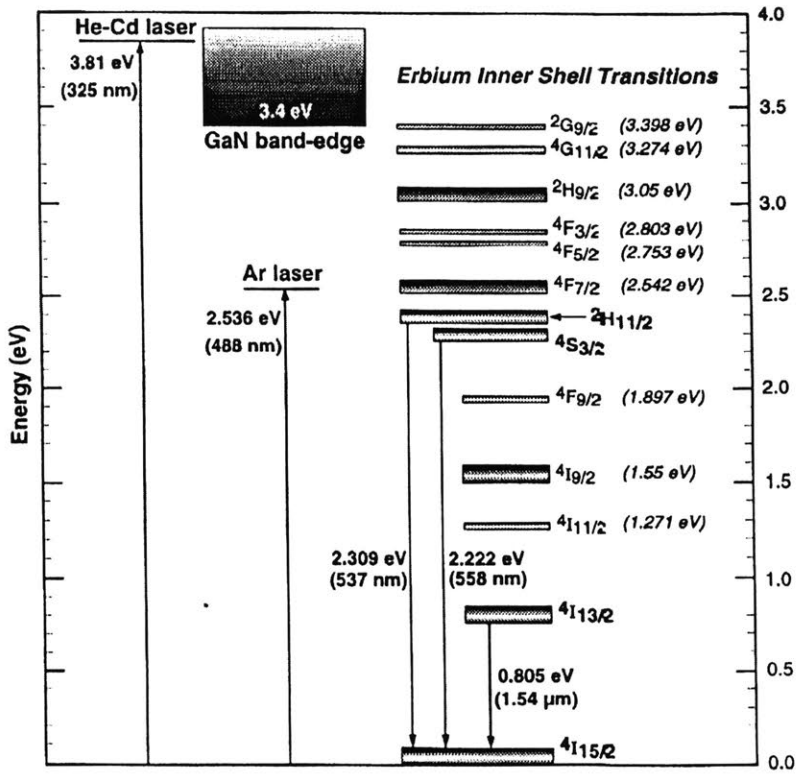

Figure 2-1: Relevant energy levels in GaN:Er photoluminescence: excitation laser photon energies, GaN conduction band edge and Er 4*f* energy levels. (From Ref. [6])

There are three methods of luminescence in Er-doped semiconductor materials. The first, described above, as the result of absorbed photon energy is photoluminescence (PL). Cathodoluminescence (CL) occurs when free carriers are created from a high-energy electron beam, and electroluminescence (EL) occurs when an electron-hole pair is created from an applied bias voltage.[5] Both CL and EL are above-bandgap Er excitation mechanisms. In this thesis GaN:Er luminescence is studied from both intra-center and above-bandgap excitation mechanisms by PL and CL.

2.1.2 Non-Radiative Erbium Emission

Thermal quenching is a result of competing non-radiative mechanisms for de-excitation that lower luminescence intensity. The non-radiative mechanism which dominates

thermal quenching above 100 K is a multiphonon absorption energy backtransfer process. This backtransfer process has been studied extensively by Taguchi *et al.*[7] and involves an intermediate Er-related energy state which binds electron-hole pairs. These bound e-h pairs can transfer their energy to the 4*f* shell by multiphonon emission or they can be returned to the bandgap energy state by absorbing phonons. The process is illustrated in figure 2-2.[1]

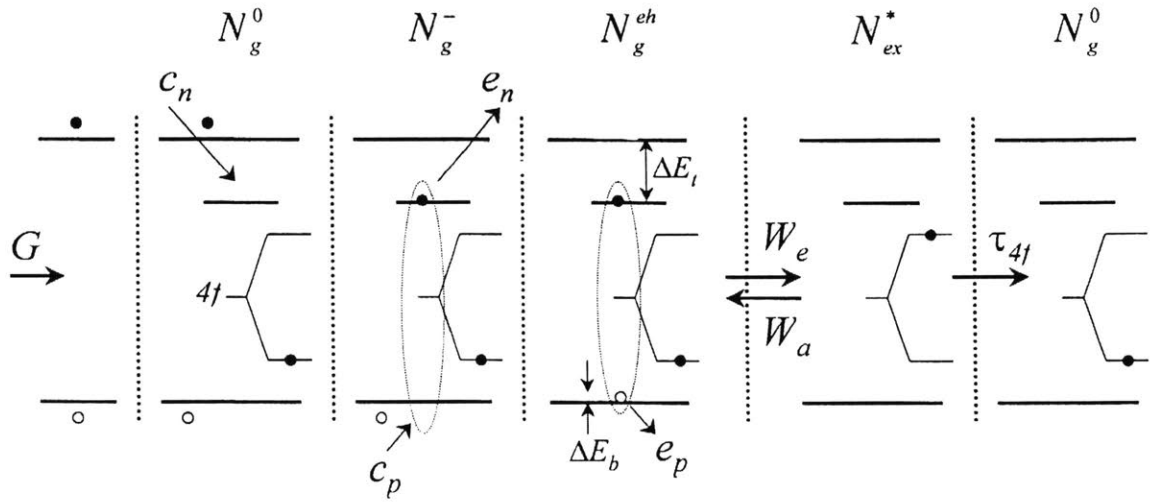

Figure 2-2: Energy transfer processes in Si:Er luminescence identified by Taguchi[7]. (From Ref. 1)

The electron emission rate is governed by the standard dependence

$$e_n \propto \exp\frac{-\Delta E_t}{kT}, \qquad (2.1)^1$$

where ΔE_t is the difference in energy between the host conduction band and the Er trap energy level. It is expected that the wider bandgap of GaN(3.4 eV compared to 1.1 eV of Si) leads to a much larger ΔE_t and thus greatly reduces thermal quenching, though this backtransfer process has not been studied in GaN:Er systems.

2.1.3 GaN:Er Growth

The GaN:Er layers are grown by Dr. Steckl at the Nanoelectronics Laboratory at the University of Cincinatti. The GaN:Er is grown by molecular beam epitaxy (MBE) using solid sources (for Ga and Er) and a plasma gas source for N_2. The use of the term epitaxy is a bit of a misnomer in this case as epitaxy refers to growth of a crystalline layer which is an extension of the substrate lattice, and Si_3N_4 and SiO_2 are amorphous. Heteroepitaxial growth, in which the grown layer and substrate have lattice mismatch has been shown to lead to many defects such as dislocations and stacking faults which form to relieve the stress from the mismatch.[8]

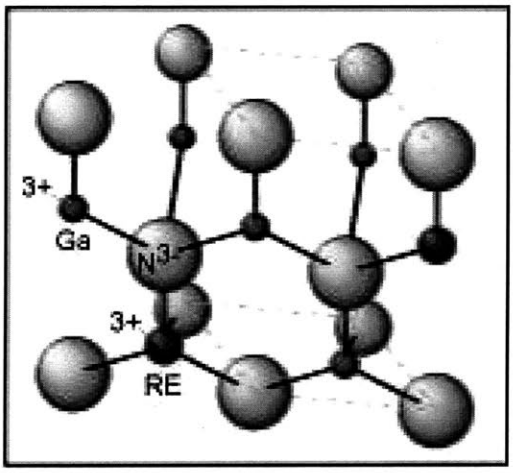

Figure 2-3: Preliminary model of the GaN:RE crystal structure. (From Ref. [5])

GaN is known to crystallize in the wurtzite structure, space group $P6_3$ mc, with lattice parameters a=0.3190 nm and c=0.5190 nm.[5] It is suggested by Steckl et al. that Er is a substitutional donor in the Ga site, with extended X-ray adsorption fine structure (EXAFS) analysis indicating an Er-N bond length of 0.217 nm, as compared to the Ga-N bond length of 0.195 nm. Incorporation of the larger Er ion in the Ga site is believed to be energetically compensated by the larger electronegativity of Er. An early proposed

model of the GaN:Er crystal structure is shown in figure 2-3. RBS channeling analysis confirms that approximately 90% of the Er atoms incorporated in the GaN lattice occupy substitutional sites even up to high concentrations of Er.[5]

While the epitaxial growth of GaN:Er layers by MBE has not been extensively studied, some clues as to the nature of the growth may be found from analysis of GaN heteroepitaxy. Brown has found that the growth of GaN by MBE leads to direct nucleation and three-dimensional island growth because the low-temperature growth of the MBE process precludes solid phase epitaxy.[9] The three-dimensional islands can be seen clearly in the high resolution TEM image of GaN grown by MBE on c-sapphire in figure 2-4. The coalescence of these islands leads to mixed threading dislocations (screw and edge).[9] The surface roughness and lack of lattice of amorphous substrates can only be expected to exacerbate this defect problem. It is believed that structural defects such as these threading dislocations, along with the stacking faults associated with heteroepitaxial growth in general, will trap the Er atoms preventing them from becoming optically active (they would be unable to undergo 4*f* transitions and emit 1.54 μm photons).

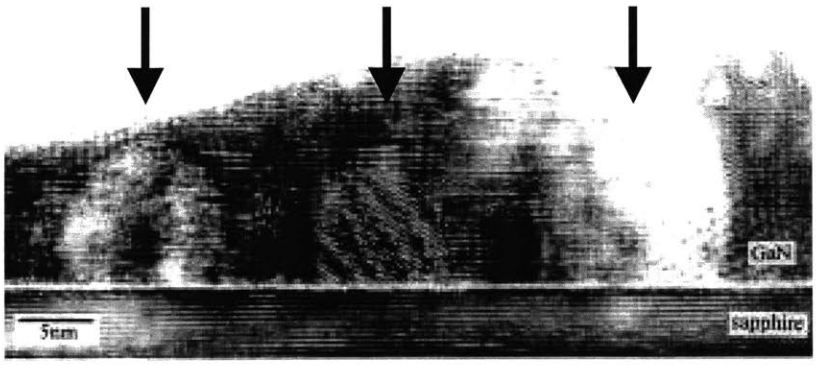

Figure 2-4. HRTEM image of three-dimensional island growth at the interface of MBE grown GaN on sapphire. (From Ref. [9])

2.2 Results and Discussion

2.2.1 Sample Preparation

Three samples were tested to evaluate the morphology and optical properties of GaN:Er grown on amorphous substrates. All layers were grown by solid source MBE by Dr. Steckl at the University of Cincinatti. The growth temperature was 600 °C, which is lower than usual for GaN:Er growth. The lower temperature was chosen to reduce the amount of oxygen impurities acting as shallow donors in the films. Typical Er concentrations in GaN:Er films grown by Steckl are on the order of 10^{20} atoms/cm^3, which is a large dopant concentration. It has been reported that O incorporation increases with growth temperature and that at 900 °C the O incorporation inhibits Er incorporation.[10] The desire for an electronically as well as optically superior growth layer requires low O incorporation, and so the choice to grow at 600 °C is necessary, despite the deleterious effect this may have on the epitaxy quality.

The reference sample is a 300 nm GaN:Er layer grown on (111)Si. The other two layers were grown on waveguide structures which will be discussed in chapter 3. These samples were fabricated by Desmond Lim and are discussed in his thesis.[11] A thermally grown SiO_2 layer on Si was then covered by a sputtered Si_3N_4 layer, which was subsequently patterned and etched into waveguide structures with feature size 800 nm (height) by 500 nm (width). A 300 nm blanket layer of GaN:Er was grown by MBE on these structures. One of the samples underwent a selective buffered oxide etch (7 HF:1NH_4OH) step to remove 100 nm of oxide prior to GaN:Er growth while the other

was not etched prior to growth. The three samples described will be referred to from here on as GaN:Er/(111)Si; GaN:Er/SiO_2, Si_3N_4, wet etch; and GaN:Er/SiO2, Si_3N_4, no etch.

2.2.2 Photoluminescence

The luminescence spectra (normalized for laser power) of GaN:Er/SiO_2, Si_3N_4, no etch; GaN:Er/SiO_2, Si_3N_4, wet etch; and GaN:Er/(111)Si are shown in figure 2-5.

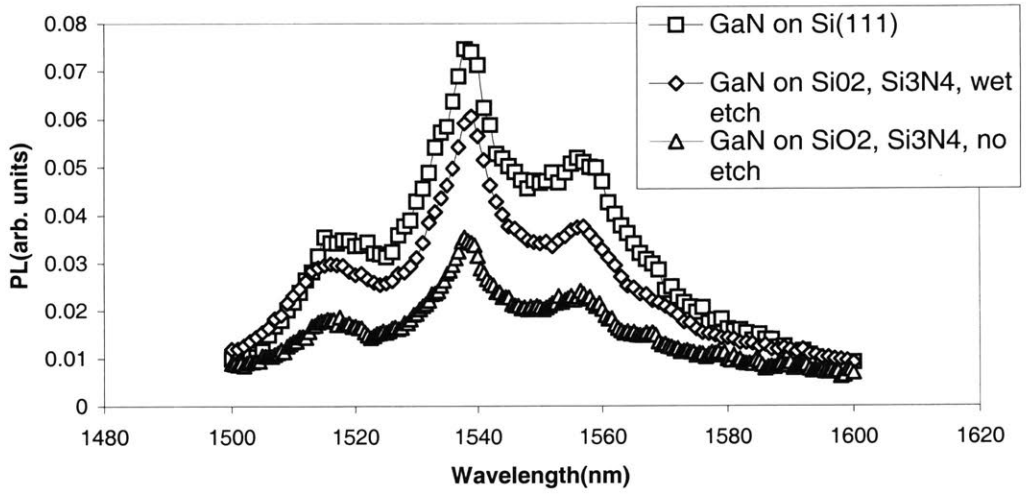

Figure 2-5: Room temperature PL of GaN/Si(111); GaN/SiO_2, Si_3N_4, wet etch; and GaN/SiO_2, Si_3N_4, no etch under 488 nm excitation from Ar^+ laser source with 40 mW power.

There are three distinctive peaks that do not change with substrate located at 1517 nm, 1538 nm, and 1557 nm. The GaN:Er grown on Si_3N_4/SiO_2 with a wet etch step gives much better luminescence than the GaN:Er layer grown on the substrate with no etch. The results are encouraging, as the GaN:Er layer grown on the wet etched substrate shows luminescence similar to that of a layer grown on a single crystal (111)Si substrate. The luminescence is essentially an indicator of the number of optically active Er sites at a given excitation power, and so the number of optically active Er sites in GaN:Er/SiO_2,

Si_3N_4 wet etch is close to the number of optically active Er sites in GaN:Er/(111)Si. This likely means that there is not as much agglomeration of Er to the defects and grain boundaries as was suspected, or it is possible that Er atoms at these sites are still optically active. Regardless, it is encouraging to see such comparable luminescence in a GaN:Er layer grown on an amorphous substrate. It is important to realize that the PL excitation is a spatially broad source and so the luminescence is an average over a large area. The Si_3N_4 structures make up a small portion of the total surface area, and GaN:Er/SiO_2 dominates the luminescence.

Saturation measurements were also taken with each sample for each of the peak wavelengths, examining the dependence of luminescence at that wavelength on laser power. None of the samples showed luminescence saturation, which indicates that even under maximum power of the laser (2W) there are still optically active Er centers which are not emitting photons.

2.2.3 Cathodoluminescence

With cathodoluminescence the electron beam can be focused to a much smaller area than the laser beam used in PL, and so the GaN:Er/Si_3N_4 can be distinguished from GaN:Er/SiO_2. Figure 2-6 shows the points examined in spot mode for GaN:Er/SiO_2 and GaN:Er/Si_3N_4 for both the wet etch and no etch samples. The spectra given in figure 2-7 show that the luminescence is stronger for the GaN:Er/Si_3N_4 than the GaN:Er/SiO_2. There is evidence that nitrided surfaces enhance epitaxial growth of GaN due to dangling N-bonds, and this may be responsible for the better luminescence of GaN:Er/Si_3N_4 compared to GaN:Er/SiO_2.[12]

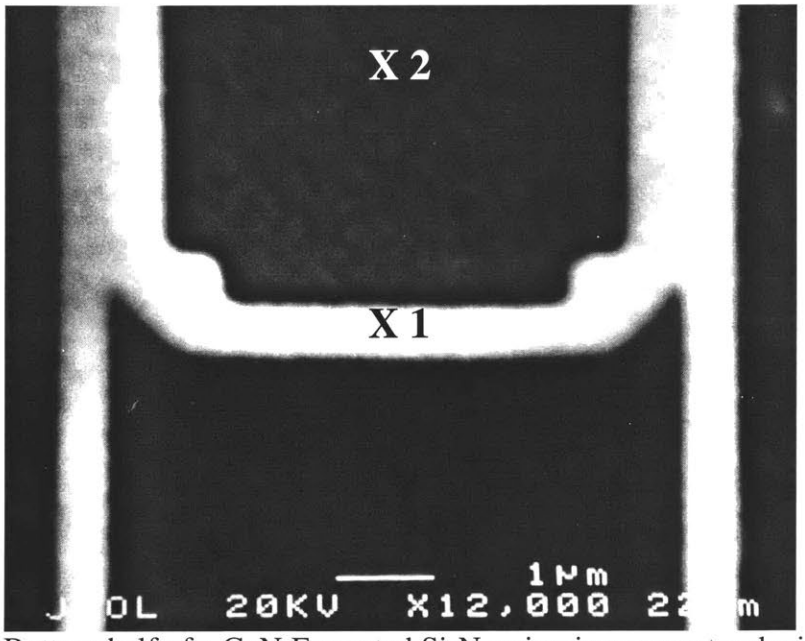

Figure 2-6: Bottom half of a GaN:Er coated Si_3N_4 micoring resonator device used for cathodoluminescence. Using spot mode a CL spectral scan was taken at X1 for GaN:Er/Si_3N_4 and at X2 for GaN:Er/SiO_2. The two measurements were taken approximately 2 μm apart.

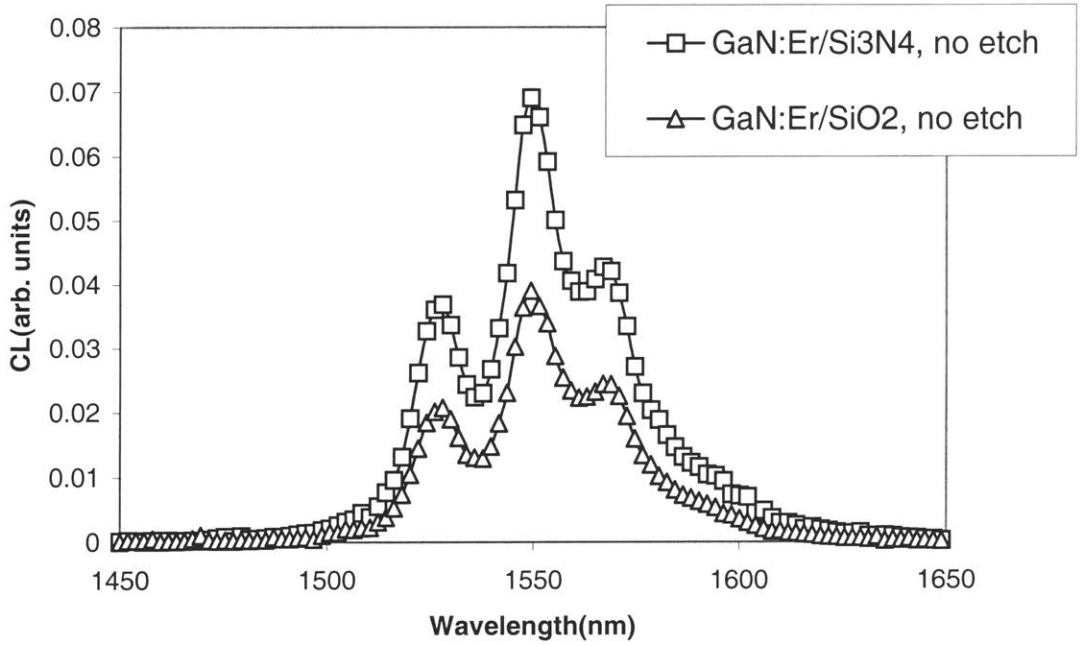

Figure 2-7: Cathodoluminescence spectra of GaN:Er/Si_3N_4, no etch and GaN:Er/SiO_2, no etch. The measurements were obtained using spot mode at the points illustrated in Figure 2-6. There appears to be a 10 nm shift in wavelength measurements due to an uncalibrated monochromator.

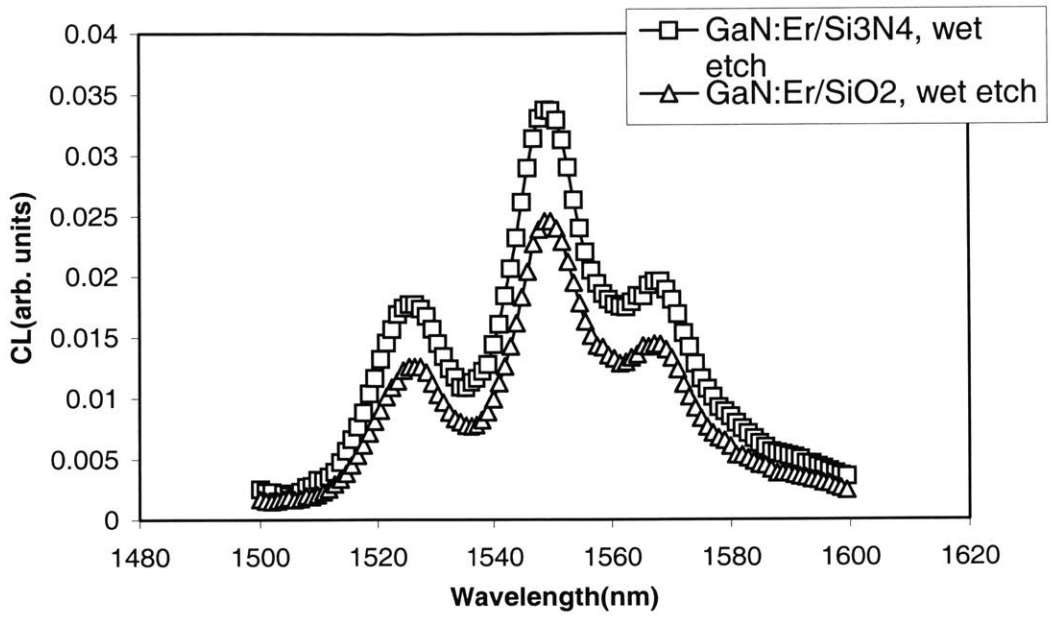

Figure 2-8: Cathodoluminescence spectra of GaN:Er/Si_3N_4, wet etch and GaN:Er/SiO_2, wet etch. The measurements were obtained using spot mode at the points illustrated in Figure 2-6. There appears to be a 10 nm shift in wavelength measurements due to an uncalibrated monochromator.

2.2.4 Atomic Force Microscopy

Atomic Force Microscopy (AFM) was used to determine the surface roughness of the GaN:Er layer grown on each of the samples. The AFM probe tip is extremely small and so it was possible to differentiate between the GaN:Er grown on Si_3N_4 and the GaN:Er grown on SiO_2. Substrate conditions prior to GaN:Er growth were reproduced and tested in an attempt to correlate substrate surface roughness with GaN:Er layer quality and surface roughness. The raster scan of a 1 μm^2 section of the GaN:Er layer on (111)Si and Si_3N_4(no etch) are shown in figure 2-9 and illustrate the variation in surface roughness resulting from growth on different substrates.

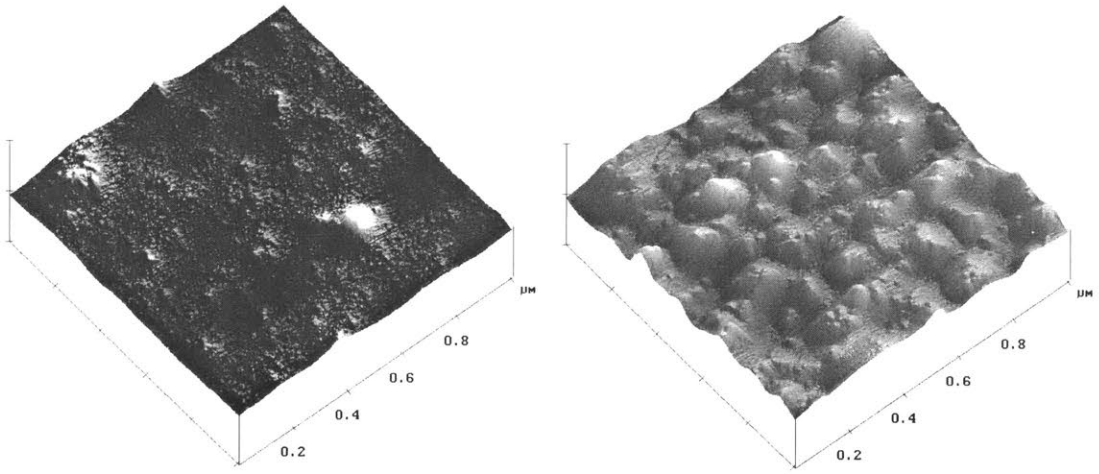

Figure 2-9: AFM images of GaN:Er surface grown on (111)Si (left), and Si_3N_4, no etch (right). The rms roughness values are 2.35 nm (left) and 9.662 nm (right).

The results of the software surface roughness analysis on all of the GaN:Er layers and their substrates is found in table 2-1, along with the PL values for each.

Table 2-1. Rms roughness values for GaN:Er layers and their substrates. PL values are included to indicate layer quality.

Sample	GaN:Er rms roughness (nm)	Substrate rms roughness (nm)	PL (λ=1538 nm, arb. units)
GaN/(111)Si	2.35	-	0.07463
GaN/Si3N4 (wet etch)	4.803	3.317	0.06058
GaN/SiO2 (wet etch)	5.316	0.324	
GaN/Si3N4 (no etch)	9.662	2.643	0.0354
GaN/SiO2 (no etch)	10.304	0.268	

The PL intensity values show that luminescence increases with decreasing surface roughness of the GaN:Er layer, which makes sense because surface roughness and defect densities should be related. CL intensity values showed much better luminescence from GaN:Er on Si_3N_4 than GaN:Er on SiO_2, indicating that growth on the rougher Si_3N_4 leads

to a better quality layer than growth on the smooth SiO_2 layer. The roughness may provide nucleating centers for GaN:Er growth, or perhaps there are dangling N-bonds which lead to a better wettability of GaN:Er on Si_3N_4 than on SiO_2. Liu *et al.* have observed that growing a thin layer of Si_3N_4 on (111)Si prior to GaN deposition is helpful because there is less lattice mismatch and better GaN adhesion, which should lower the concentrations of dislocations at the interface.[12] The wet etch step has a highly beneficial effect on GaN:Er growth as the GaN:Er grown on the wet etched substrate has a lower surface roughness and higher photoluminescence than the GaN:Er grown on the non-etched substrate. This may be due to a cleaning effect, reducing the impurities at the surface, or it may affect the surface chemistry.

2.3 Future Work

2.3.1 GaN:Er Growth Analysis

The comparable PL of the wet etched sample to the (111)Si substrate sample is highly encouraging, but a better understanding of why the wet etch and Si_3N_4 substrates are preferable could lead to further surface engineering to grow even better GaN:Er layers. Transmission Electron Microscopy (TEM) images of the GaN:Er/substrate interface could help us better understand the growth process taking place.

2.3.2 Growth on Unpatterned Si_3N_4

The growth on the Si_3N_4 is not as well defined as the growth on the SiO_2 because of the smaller growth area. In chapter 3 a structure is suggested which involves growth of GaN:Er on a planar Si_3N_4 substrate, so it would be useful to obtain data on such a layer.

2.3.3 Defect Analysis

It has been shown that GaN:Er grown on amorphous substrates gives comparable PL to GaN:Er grown on (111)Si, however, the question of why this is has still not been answered. The interaction between defects and Er atoms is not well understood, and should be explored. TEM images could be used for this analysis as well.

2.4 Conclusion

High quality GaN:Er layers have been grown on amorphous substrates of patterned Si_3N_4 waveguide structures on SiO_2 which show comparable room temperature photoluminescence to GaN:Er grown on (111)Si. It appears that Si_3N_4 is a better choice for substrate than SiO_2, and that surface modifications as a result of a (7 HF:1 NH_4OH) wet etch are beneficial to GaN:Er growth. Surface roughness values seem to be an indicator of layer quality as the least rough surfaces showed the best PL, though GaN:Er/Si_3N_4 showed superior CL to GaN:Er/SiO_2 with similar surface roughness values. The ability to grow high-quality GaN:Er layers on amorphous substrates opens the door for GaN:Er use in electronically-pumped optical amplifiers operating at room temperature such as microring and microcavity resonators, which are discussed in the following chapters.

Chapter 3

Microring Resonators with GaN:Er Core

3.1 Background

The GaN:Er layer grown on Si_3N_4/SiO_2 waveguide structures has been shown to give good 1.54 μm luminescence. The first microresonator structure considered is the microring resonator.

3.1.1 Waveguiding

The basic building block of microphotonics is the waveguide, which is the optical analog of the electrical wire. The important materials property to consider in waveguide design is the refractive index, n, which is defined by:

$$n = \frac{c}{v} = \sqrt{\frac{\varepsilon\mu}{\varepsilon_0\mu_0}} \qquad (3.1)^{13}$$

where c and v are the speed of light in vacuum and the given material, respectively. ε_0 and μ_0 are the permittivity and permeability of vacuum, and ε and μ are the permittivity and permeability of the given material. The refractive indices of materials commonly used in waveguides are listed in table 3-1.

Table 3-1. Refractive indices of materials commonly used in waveguiding.[11]

Material	Si	SiO_2	Si_3N_4	Air
Refractive Index, n	3.5	1.5	2.0	1

A basic understanding of waveguiding can be gained by following the 2-D, ray optics approach with light traveling between two perfectly reflecting mirrors presented in Saleh.[14] Snell's Law describes how light propagates at an interface of materials with differing n:

$$n_i \sin\theta_i = n_t \sin\theta_t, \qquad (3.2)^{13}$$

where θ_i and θ_t are the angles between the normal to the interface and the ray of the incident and transmitted light. If θ_t is 90° then there will be total internal reflection and no transmitted wave. From this it can be shown that total internal reflection will result when:

$$\theta_i \geq \sin^{-1}\frac{n_t}{n_i}. \qquad (3.3)^{14}$$

The light ray is now modified to more accurately represent the light wave as a transverse electromagnetic wave with a **k** vector in the direction of the light ray and with magnitude $1/\lambda$. Waveguides are designed for TE modes where the electric field is transverse to the direction of propagation, so for this simplified problem we can ignore the magnetic field. Interference of the electric field dictates that only discrete values of θ_i will lead to constructive interference and propagate down the 2-D waveguide as shown in figure 3-1. The θ_i which lead to constructive interference (Figure 3-1b.) give the real modes that will propogate in the waveguide. These θ_i obey the equation

$$\theta_i = \cos^{-1}\frac{d}{n\lambda}, \qquad (3.4)^{14}$$

as well as (3-3). The propagation constant is defined as

$$\beta = d \cdot \cot\theta_i, \qquad (3.5)^{14}$$

and the speed in the z-direction of the light wave is equal to βv.

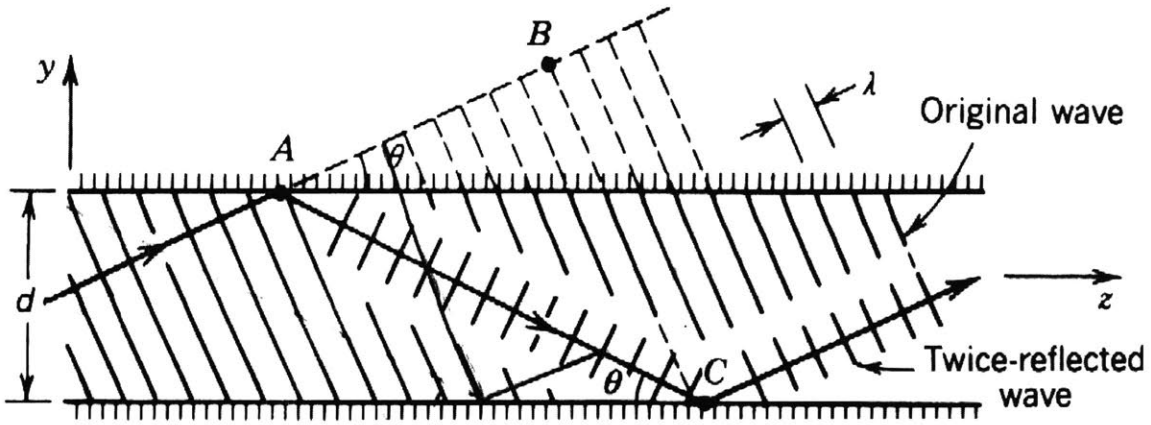

a)

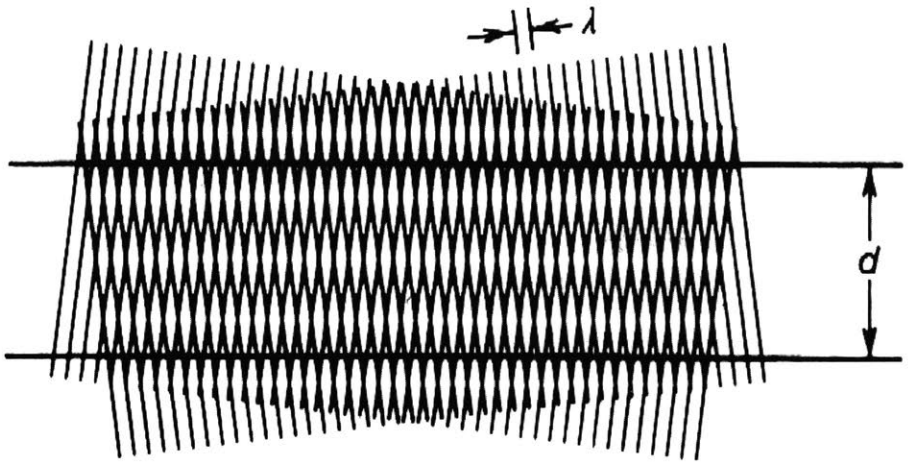

b)

Figure 3-1. Simplified 2-D waveguide with light propagation in the z-direction (a), and the resulting interference pattern with allowed θ_i(b). (From Ref. [14])

Light waves that carry information are often sent as pulses to represent digital information. If one bit is sent and then the next is sent at an incident angle corresponding to a larger β then the second bit will reach the signal processor first and the data will be lost. To keep these pulses in the correct order they must travel at the same speed, which can only be achieved by designing a waveguide that only allows one θ_i. Such a waveguide is called a single mode waveguide, and can be made by decreasing d

until only one value of incident angle θ_i satisfies both (3.3) and (3.4).[14] The 2-D problem solved above can be extended to more complex 3-D structures using the effective index method, illustrated in figure 3-2, where average indices n_1, n_2, and n_3 are determined and the problem again becomes 2-D.[11]

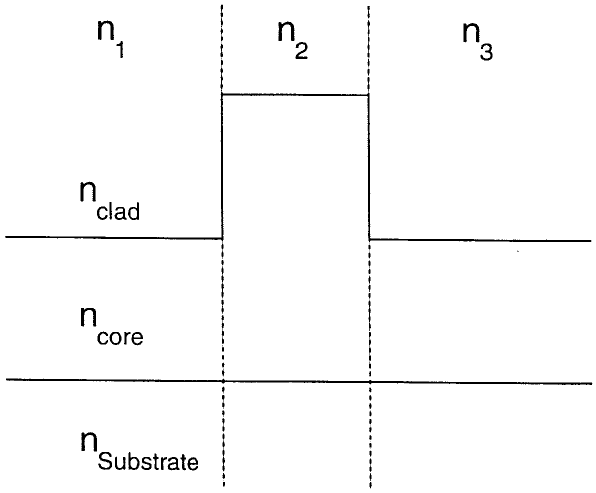

Figure 3-2: Illustration of the effective index method on a ridge waveguide structure. An average index is determined for each section by averaging n_{clad}, n_{core}, and $n_{substrate}$ for that section. The problem is then reduced to a 2-D slab waveguide with core n_2 and cladding n_1, n_3. (From Ref. [11])

The Apollo Optical Waveguide Mode Solver software package employs this method, and was used to run simulations on different waveguide designs discussed later in this chapter.

3.1.2 Microring Resonators

Resonator structures have been shown to enhance the spontaneous emission of specific wavelengths which correspond to the resonant frequency of the resonator. The equation that governs this enhancement is

$$\eta = \gamma \frac{Q}{\left(\frac{V}{\lambda^3}\right)}, \qquad (3.6)^{15}$$

where η is the enhancement factor, γ is a constant, Q is the quality factor of the resonator, V is the ring volume, and λ is the wavelength that is being enhanced. The resonant frequency can be tuned to enhance Er 1.54 μm emission. A microring resonator consists of two straight waveguides which couple light into and out of a circular waveguide (ring), as shown in figure 3-3.[11]

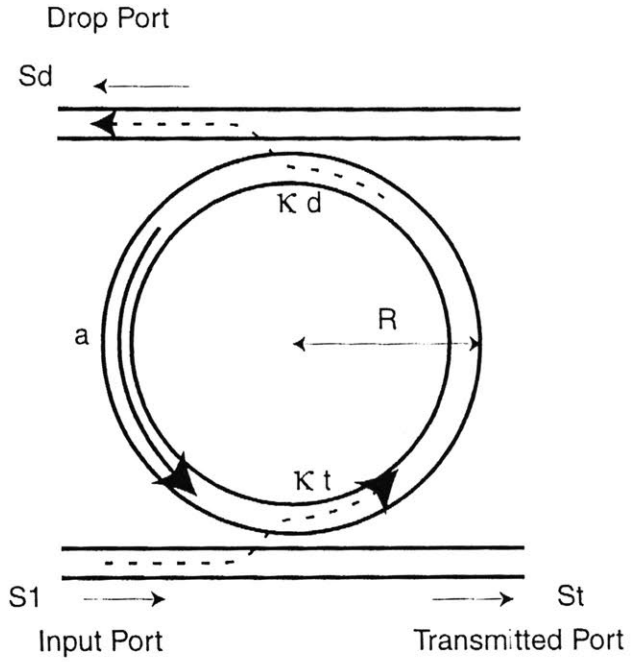

Figure 3-3: Schematic of a microring resonator. Light traveling through the input port is coupled into the ring of radius R, and eventually couples out of the ring into the drop port. (From Ref. [11])

The circumference of the ring is chosen to be an integer multiple of the desired wavelength for enhancement. A standing wave is set up in the ring and wavelengths other than the resonant wavelength will destructively interfere. As seen in (3.6) enhancement of the emission is proportional to the resonator quality factor,

$$Q=\frac{\lambda}{\Delta\lambda}, \qquad (3.7)^{11}$$

where λ is the resonant wavelength and $\Delta\lambda$ is the full width at half maximum (FWHM) of the resonant peak. The microresonators used in this section were studied extensively (without GaN:Er) by Desmond Lim and microring resonator Q values on the order of 1000 were obtained.[11]

3.1.3 Waveguide Design

The waveguide structures used in this section are channel waveguide structures which have tightly confined modes and incur low bending losses. The channel waveguide structure used is shown in figure 3-4.

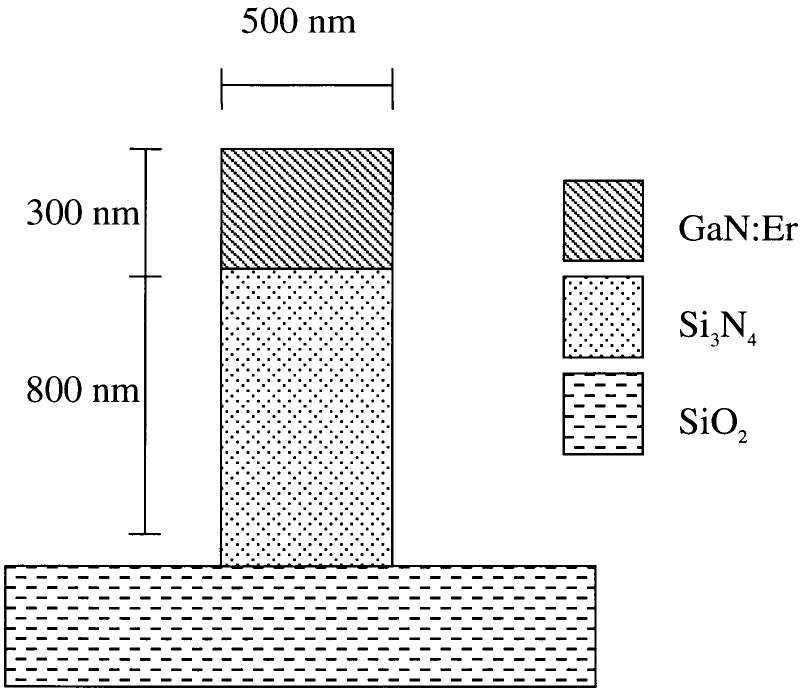

Figure 3-4: Channel waveguide structure used in this thesis. The light mode should be confined in the top, higher-index, GaN:Er layer.

Light is confined in the core because it has a higher refractive index (2.3 literature[16], 2.1 measured) than the air (1.0) and Si_3N_4 (2.0) cladding surrounding it.

The ridge waveguide structure does not confine the mode as tightly as the channel waveguide but has other advantages that will be discussed later. The standard structure

of a ridge waveguide is shown in figure 3-5. The average refractive index of the middle section is higher than the outer section because of the ridge of height h and width w. The mode is confined in the middle section because of this index difference.

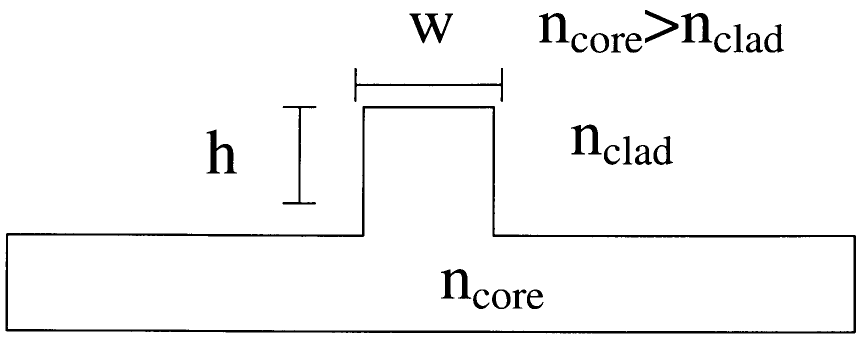

Figure 3-5: Ridge waveguide structure. The ridge of height, h, and width, w, gives the middle section a higher index and the mode is confined in this middle section.

The horizontal confinement of the mode can be improved by increasing h, which leads to a higher index contrast between the center and outer sections.

3.1.4 Surface Roughness Losses

Surface roughness, which was discussed in chapter 2, is a concern for waveguides because it is a significant source of loss for waveguides with submicron widths. Lee has studied sidewall roughness loss in the Si/SiO_2 system extensively, and has found that the two important parameters are the rms roughness (σ) and the contour length (L_c).[17] The contour length describes the periodicity, and in this case is approximately the grain size. Loss has been found to increase linearly with σ, while it reaches a maximum at

$$L_c=\lambda/4n. \qquad (3.8)^{17}$$

It has also been found that loss due to interface roughness is proportional to the index contrast cubed (Δn^3).[18]

3.2 Results and Discussion

3.2.1 Sample Preparation

The two device samples described in chapter 2 each contained many devices which were organized into four sections. The samples were die sawed into device sections and facets were polished. The polishing procedure was the same as has been used on Si/SiO_2 waveguides, and involves aligning the sample and polishing with 1 μm, 0.3 μm, and finally 0.1 μm paper.

3.2.2 Transmission Testing

A tunable NaCl laser coupled to a lens-tipped optical fiber was used to couple light into the waveguide structures. The output was measured with a Ge photodectector. Transmission loss measurements were attempted on the waveguides but output light was not detected, even when the sample was pumped by a 980 nm laser, indicating that there is significant transmission loss occurring somewhere along the light path. The first possibility is that the light is not being efficiently coupled into the waveguide, which could be the result of a poor quality polished facet. Another possibility is that the waveguide is lossy, perhaps from surface or sidewall scattering. Lastly, it is possible that the waveguides were damaged too severely during GaN:Er growth or prior to deposition and so the input and output were not connected which would lead to no output signal.

3.2.3 Scanning Electron Microscopy

SEM was used to examine the broken waveguide structures, and because of its nature gives insight as to when the damage occurred. The broken waveguide structure in figure 3-6 (left) appears extremely bright because it is disconnected from the rest of the layer and is charging since there is no conducting path for the incident electrons. The dark

portion of the waveguide appears to show a trench into the GaN:Er layer. This was confirmed by AFM and indicates that the Si_3N_4 waveguide broke off after GaN:Er was already deposited. The bright fragmented piece above the ring resonator further supports this and is likely from one of the nearby trenches.

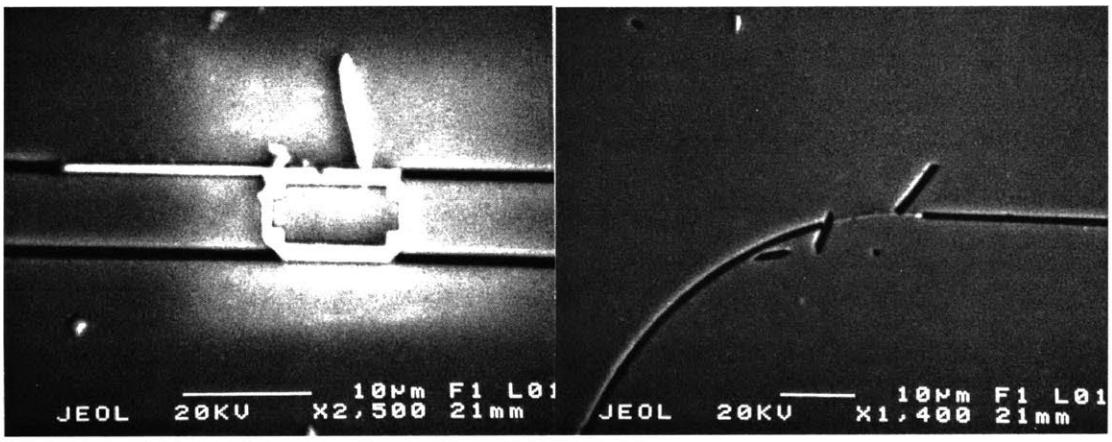

Figure 3-6: SEM images of broken waveguide structures from GaN:Er/SiO_2, Si_3N_4, wet etch at magnification 2500X (left) and 1400X (right).

The broken waveguide in figure 3-6 (right) is dark throughout and the trench appears smaller, indicating that this waveguide was most likely broken before GaN:Er deposition. Possible reasons for the breakage include undercutting from the wet etch, thermal mismatch during GaN:Er growth (600 °C), or even handling during facet polishing. It is clear that the structures are very fragile, and that a better structure must be designed to increase the yield of usable devices.

3.2.4 Surface Roughness Concerns

The morphology of the GaN:Er layers was examined in chapter 2, and values of rms roughness (σ) and contour length (L_c) were obtained. The relevant values for waveguide loss calculations are summarized in table 3-2. The rms roughness value of the

Table 3-2: Relevant surface roughness values determined by AFM of GaN:Er waveguide structures.

Sample	Rms roughness (nm)	Contour length (approx., nm)
GaN:Er/Si3N4, wet etch	4.803	150
GaN:Er/Si3N4, no etch	9.662	200

GaN:Er/Si_3N_4, wet etch is similar to that of measured sidewall roughness for Si waveguides. It can be assumed that sidewall roughness values for the GaN:Er waveguide sections is of similar magnitude, and so now the loss due to waveguide roughness is approximately double that of single crystal or amorphous waveguides since GaN:Er has both sidewall and surface and substrate roughness as well. Perhaps most troubling is the L_c values, which are extremely close to the value for maximum loss defined by $\lambda/4n$ (3.8), which in the GaN:Er case has a value of L_c=180 nm. Growth at a temperature even lower than 600 °C would lead to a larger L_c, while growth at a higher temperature would lead to a smaller L_c. Because of the O incorporation problems discussed earlier it would be best to try growth at a lower temperature to see if that positively effects the L_c value. The fact that loss is proportional to $(\Delta n^3)^{18}$ suggests that a non-air clad structure, such as a ridge waveguide, could reduce the problem of surface roughness scattering loss significantly, without changing the growth conditions. Such a structure is designed and proposed in the next section.

3.2.5 Apollo Simulations

The Apollo Optical Waveguide Mode Solver software package can be used to simulate the possible modes of light transmission in a given waveguide structure. The refractive

index of Si_3N_4 fabricated at Lincoln Labs is reported by ellipsometry as 2.4, which is much higher than the expected 2.0.[16] This unfortunate problem has since been remedied, and so it makes sense to design future structures using the value n=2.0 for Si_3N_4. The refractive index of GaN:Er was found to be 2.1 from a microcavity reflectance sprectrum (see 4.2.2). The original design of the channel waveguide structure makes sense as the literature values of n for GaN and Si_3N_4 of 2.3 and 2.0[16], respectively, would lead to good confinement of the mode in the GaN:Er layer. However, with the actual GaN and Si_3N_4 n values of 2.1 and 2.4, the mode is confined in the Si_3N_4. This means that even if we did find an output signal we would only be testing the effect of GaN:Er cladding on a Si_3N_4 waveguide. No enhancement would be seen because photons would not be traveling through the GaN:Er layer.

Surface roughness loss is a concern due to the polycrystalline nature of the GaN:Er growth, and so a ridge waveguide structure is proposed to minimize this loss. By burying the GaN:Er layer under a low index contrast Si_3N_4 layer, the effects of surface roughness loss are reduced considerably (loss is proportional to $(\Delta n)^3$). This structure has many advantages over the current channel waveguide structures. The GaN:Er layer is deposited on Si_3N_4, which has been shown to be the best cladding substrate. The GaN:Er layer thickness has been doubled to 600 nm, to allow for a larger mode and easier coupling. No patterning of the GaN:Er layer is necessary, and the deposition of the top Si_3N_4 layer should protect the fragile GaN:Er layer and reduce surface roughness losses. Lastly, the patterned Si_3N_4 structures are no longer subject to thermal stresses due to GaN:Er growth, as they are now fabricated after this step.

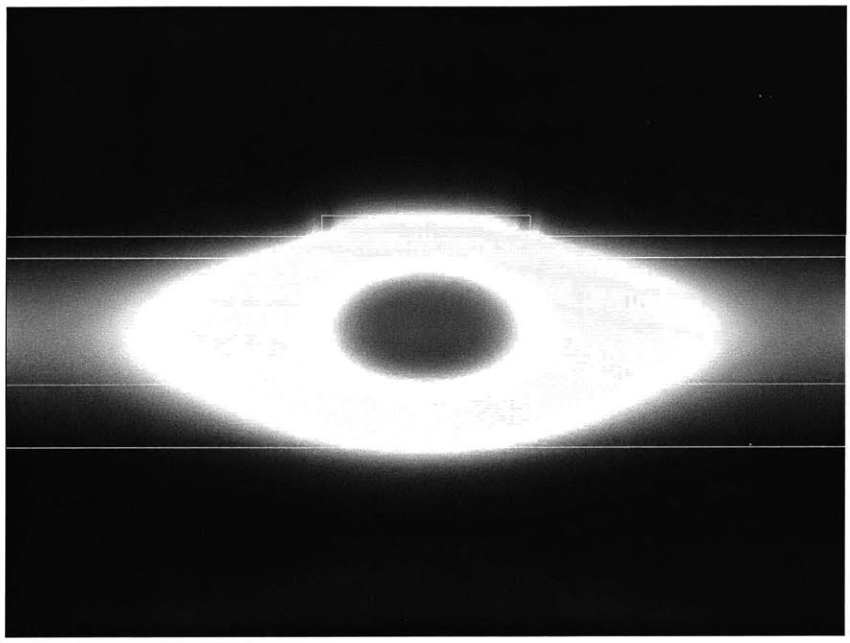

Figure 3-7: Apollo simulation of proposed ridge waveguide structure. The light is confined primarily in the middle GaN:Er layer. The ridge in this structure is 100 nm high and 2500 nm wide to give the largest mode to allow for easier coupling.

The ridge waveguide structure also allows for many design modifications to address specific device needs. By increasing the width of the ridge, w, to the single mode limit of 2.5 um you can maximize the mode size and therefore improve coupling efficiency. However, you would then need a higher pump power to create a population inversion throughout the device (enhancement is inversely proportional to cavity volume V, (3.6)). If bending loss is a concern then mode confinement can be improved by increasing the ridge height, h. However, this will also pull some of the guided mode up into the Si_3N_4 ridge, which will lower enhancement. Each of these parameters must be chosen carefully with the device needs in mind to design the optimal structure. Figure 3-7 shows the optimal design for a straight waveguide with the largest possible single mode. This waveguide has a low h to provide maximum confinement within GaN:Er, and the single mode limit for w of 2.5 μm to allow for the easiest coupling.

3.3 Future Work

Clearly, there are many hurdles to the successful use of GaN:Er layers in waveguide structures such as the microring resonator. The proposed ridge waveguide structure will mitigate most of the problems such as waveguide breakage and surface roughness scattering losses. These ridge waveguide devices should be fabricated and studied to see if transmission losses are lessened and transmission is possible in both straight and bent waveguides using GaN:Er layers.

3.4 Conclusion

The microresonator samples studied with GaN:Er did not work for many reasons. Surface roughness and L_c values indicate that GaN:Er channel waveguides are quite lossy, with other problems such as coupling efficiency and waveguide breakage further complicating the issue. Chapter 2 proved that making waveguide structures with GaN:Er cores is possible due to the discovery of an acceptable cladding material, however, chapter 3 has shown that GaN:Er waveguide fabrication is difficult. The proposed ridge waveguide structure provides a good solution to many of the problems encountered in this chapter.

Chapter 4

Microcavity Resonator with GaN:Er Defect Layer

4.1 Background

4.1.1 Microcavity Resonators

The microcavity resonator, like the microring resonator, can be used to enhance spontaneous emission at the Er emission wavelength 1.54 μm. This enhancement is due to an increase in the optical mode density around the resonant frequency of the cavity, as shown by Chen (figure 4-1).[1]

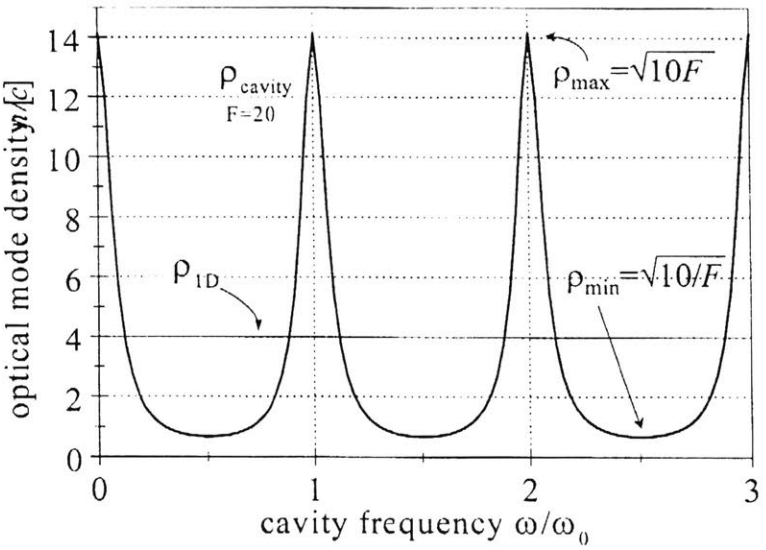

Figure 4-1: Optical mode density for a one-dimensional cavity (ρ_{cavity}) and for a one dimensional homogeneous medium (ρ_{1D}) versus frequency. The average emission enhancement (or suppression) is given by the ratio ($\rho_{cavity} / \rho_{1D}$). The maxima in the mode density correspond to the resonant frequencies of the cavity. (From Ref. [1])

A microcavity consists of a luminescent defect layer sandwiched between two distributed Bragg reflectors made from periodic dielectric stacks of alternating high and low n materials. The reflectance of the dielectric mirror can be understood as a result of the constructive and destructive interference of the multiple reflections that occur at each interface. By adjusting the thicknesses of each of the layers a photonic bandgap can be created such that no photon modes over a certain wavelength range can propagate in the material.[1]

The photonic bandgap (PBG) is analogous to the electronic bandgap and refers to energy states of photons that are forbidden in the material. Just as defects in an electronic material can allow intra-band trap states, a defect layer in the dielectric stack can lead to a defect energy state within the PBG. This defect energy state is a resonant mode of the cavity defined by the two mirrors on either side of the defect layer and can be tuned by varying the thickness of the defect layer. It can be shown that the maximum reflectance occurs for layers with thickness $\lambda/4n$, and that maximum enhancement occurs for a defect layer of thickness $\lambda/2n$.[1] The reflectance spectrum and photonic band diagram for a Si/SiO_2 reflector with a $\lambda/2n$ Si:Er defect layer are shown in figure 4-2.

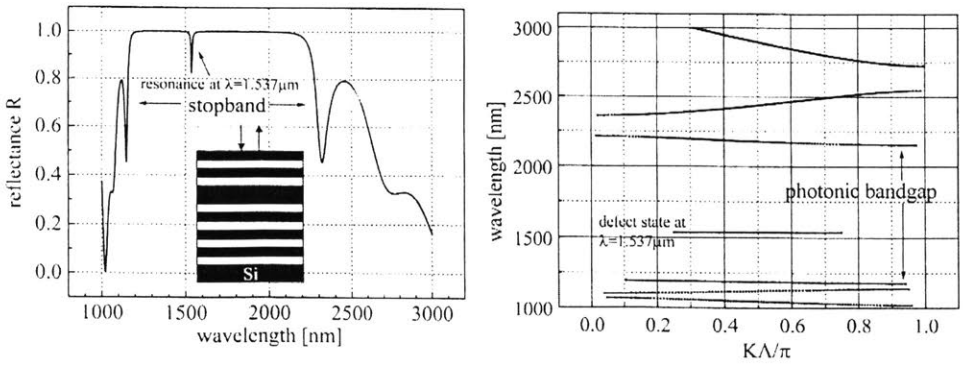

Figure 4-2: Reflectance vs. wavelength at normal incidence for a microcavity on a Si substrate with a resonant state at λ=1.54 μm (left) and the corresponding PBG diagram for the microcavity, showing a defect state in the middle of the PBG. (From Ref. [1])

4.2 Results and Discussion

4.2.1 Open Cavity Photoluminescence

The microcavity sample studied was prepared by depositing 4 pairs of a-Si/a-SiO2 (110/256 nm) on a silicon substrate. The GaN:Er layer was then grown by MBE at the University of Cincinnati. Room temperature PL was then taken for this structure with Ar^+ laser (488 nm) intra-center excitation to determine the quality of the GaN:Er film grown on amorphous silicon. The spectrum obtained is shown in figure 4-3 and shows the same peaks as were seen with GaN:Er on (111)Si and the SiO_2/Si_3N_4 substrates. This demonstrates that the film is of good quality and that the finished microcavity tuned to 1.54 μm should show enhancement of the middle Er peak.

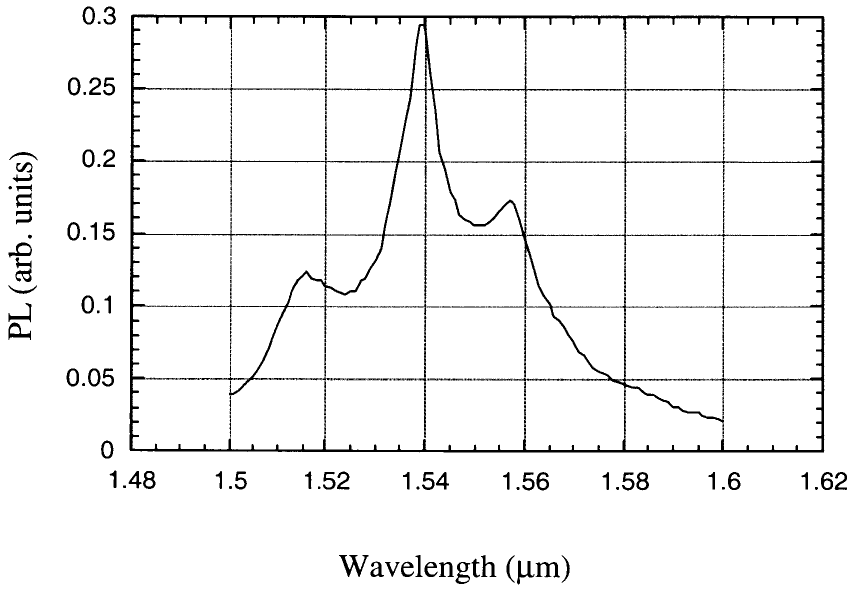

Figure 4-3: Photoluminescence spectrum of GaN:Er open-cavity structure under excitation by Ar^+ laser (λ=488 nm).

4.2.2 Microcavity Reflectance

A TEM image of the open cavity indicates that the GaN:Er layer is 380 nm thick, which is thicker than the desired $\lambda/(2n)$ thickness of 334 nm. However, the value of 334 nm was determined using the literature value of 2.3 for GaN refractive index, which we have determined to actually be 2.1. Using 2.1 for n_{GaN} gives a desired thickness of 367 nm, so our layer is still too thick.

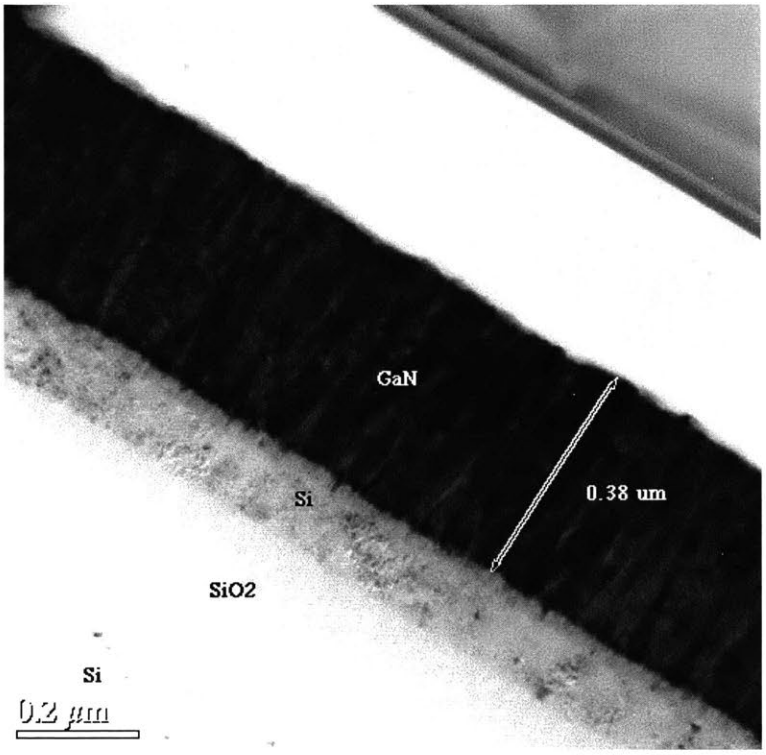

Figure 4-4: TEM image of GaN:Er open cavity. The GaN:Er layer thickness is 380 nm.

This should shift the resonant peak to a value larger than 1.54 μm. It is also important to note that due to the polycrystalline nature of the layer that the thickness is not uniform, which should broaden the resonant peak as the peak will be an average over all of the thickness variations. This is not ideal as Q will be decreased in this case and enhancement is not maximized.

Two more pairs of a-Si/a-SiO2 (110/256 nm) were deposited on top of the GaN:Er layer to complete the microcavity structure, with two corners masked to preserve the open cavity condition. A relative reflectance spectrum was obtained by Fourier Transform Infrared Spectroscopy (FTIR) and is shown in figure 4-5. As expected, the resonance at 1.56 um and 1.58 um is larger than the desired 1.54 um. It is still possible for the microcavity to enhance the Er peak at 1557 nm. The resonant frequencies can be used along with the defect layer thickness obtained with the TEM image to calculate a refractive index value of 2.09 +/- 0.02 for GaN:Er, which is smaller than the reported value. This is the first precise determination of refractive index for GaN:Er, as far as we know.

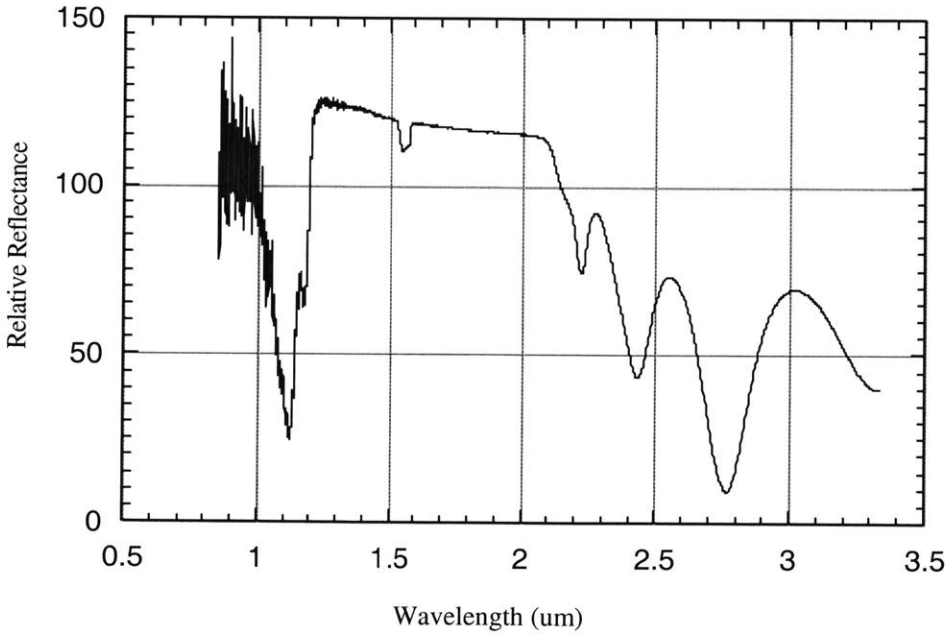

Figure 4-5: Relative reflectance spectrum of microcavity with GaN:Er defect layer obtained by Fourier Transform Infrared Spectroscopy (FTIR).

4.2.3 Microcavity Cathodoluminescence

It was not possible to obtain PL for the GaN:Er microcavity sample because the Ar^+ laser (488 nm) is reflected by the top dielectric mirror. A scattering matrix calculation method was used to obtain the calculated reflectance spectrum shown in figure 4-6, which shows the high reflectance at 488 nm.

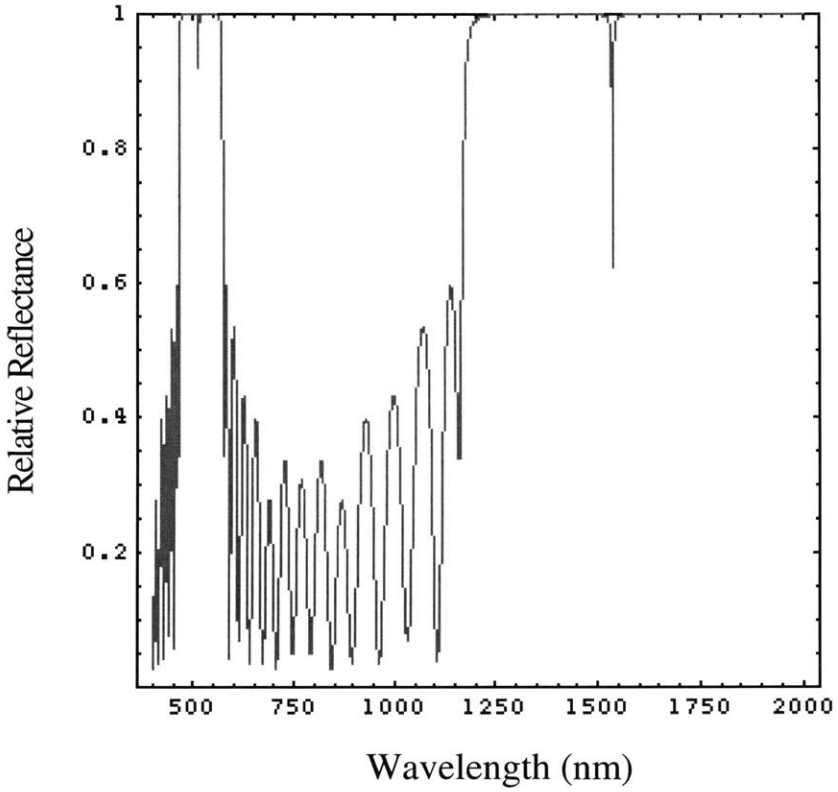

Figure 4-6: Reflectance spectrum for our microcavity calculated by the scattering matrix method. The calculations show that photoluminescence with Ar^+ laser (488 nm) excitation should be impossible, which was confirmed by the weak PL we observed.

CL is not affected by the dielectric mirrors because the excitation is from an electron beam. The CL spectra obtained using raster mode for both the open cavity corner and the center microcavity section of the sample are shown in figure 4-7. The peak shift of 10 nm is attributed to the non-calibrated monochromator, since the spacing between peaks is

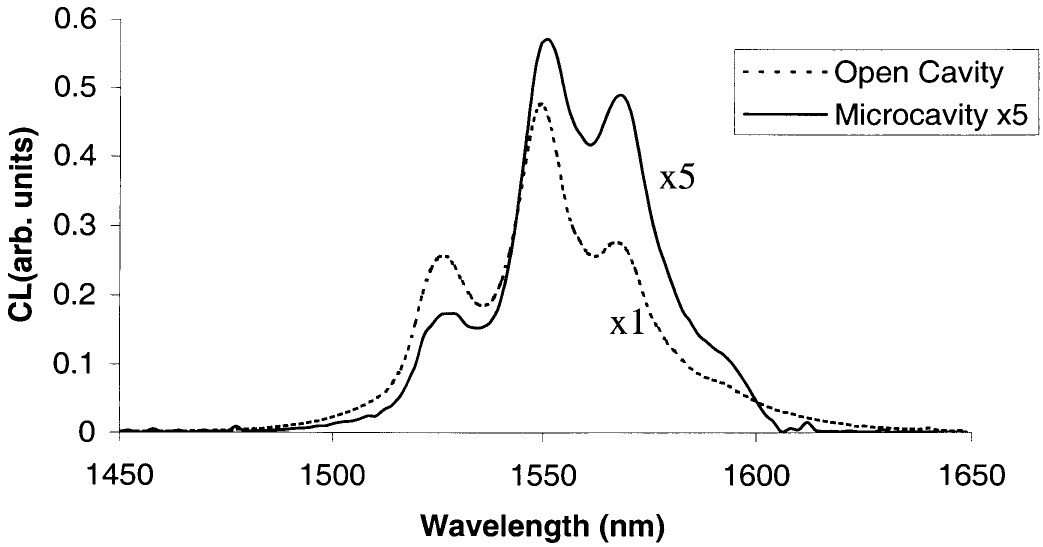

Figure 4-7: Cathodoluminescence spectrum for open cavity and microcavity samples. The microcavity luminescence was increased 500% to show the distortion of the microcavity spectrum compared to the open cavity spectrum.

the same as seen in PL spectra. These spectra show a distorted luminescence spectrum, with a higher intensity of the 1557 nm peak in the microcavity section, and a lower intensity of the 1517 peak, which indicates that the microcavity structure does affect the luminescence of the GaN:Er layer. The CL of the microcavity is weaker than that of the open cavity because the broad transmittance peak at 1.56-1.58 μm is not very large. In fact, the relative reflectance spectrum shows that only about 10% of the light at those wavelengths should be transmitted. The fact that so much luminescence is seen at these wavelengths suggests that the microcavity is enhancing luminescence.

The last feature of the CL spectra to note is that there is not a single, sharp, enhanced wavelength, but rather that much of the 1500-1600 nm range appears enhanced. This is due to the broad collection angle of the mirror used by the SEM to direct photons to the photodetector.

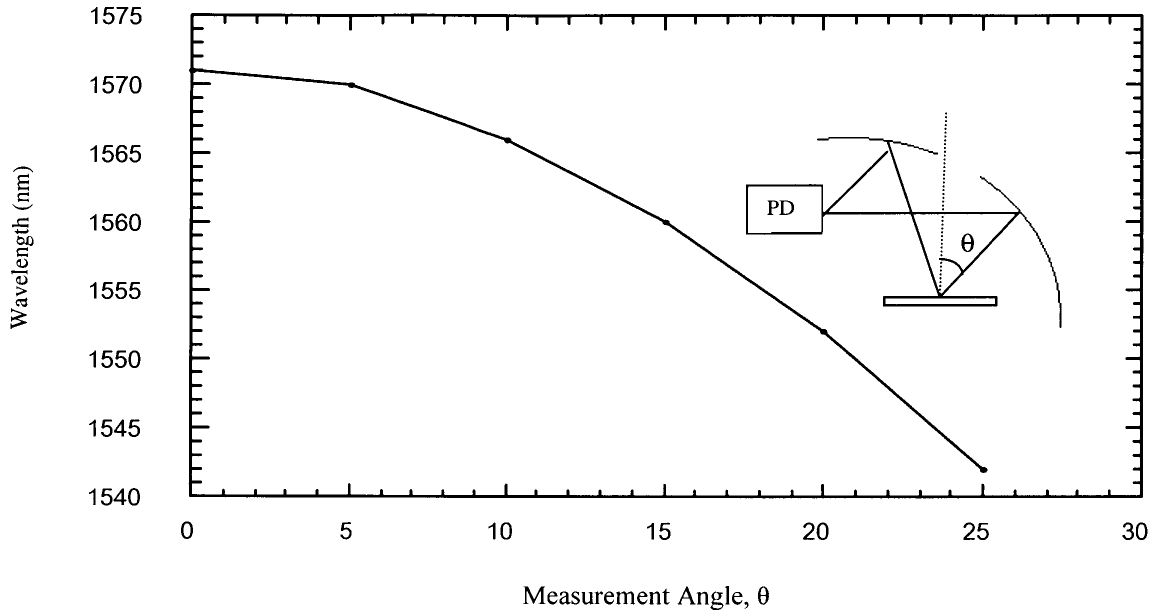

Figure 4-8: Calculated shift of resonant wavelength with measurement angle. The inset schematic of the SEM collection mirror illustrates the broad collection angle of the photodetector.

The enhanced wavelength is shown to shift to shorter wavelength values as the collection angle is shifted from the normal. This explains the broadly enhanced spectrum.

4.3 Future Work

The microcavity resonator needs to be altered so that its luminescence can be studied under intra-center Ar^+ laser (488 nm) excitation. This can be achieved by changing the number of dielectric pairs in the mirrors to shift the reflectance spectrum and allow 488 nm transmission. In the meantime the microcavity should be examined under excitation from a 980 nm GaAs laser.

The layer thickness was not optimized, and another should be grown to see if precise thickness GaN:Er layers can be grown by MBE. This should be possible, and so the only remaining problem is the thickness variation. There is a tradeoff between layer

thickness specificity and layer thickness uniformity if an etch process is used, but this possibility should be investigated.

4.4 Conclusion

The microcavity showed the ability to distort the luminescence spectrum of GaN:Er, suggesting enhancement. The GaN:Er layer is not the optimal thickness, and so the resonant peak was shifted from the desired wavelength of 1.54 μm to 1.56-1.58 μm. The broad resonance is a result of the thickness non-uniformity of the GaN:Er defect layer, and resulted in a weakened transmission of the enhanced wavelengths. Under more optimal testing conditions, and with an improved uniformity of the GaN:Er layer, enhancement of the 1.54 μm Er peak should be seen at room temperature.

Bibliography

[1] Thomas D. Chen, *Energy Transfer and Luminescence Enhancement in Er-doped Silicon,* PhD Thesis, MIT, 1999.

[2] A. J. Steckl and J. M. Zavada, "Optoelectronic Properties and Applications of Rare-Earth-Doped GaN," *MRS Bulletin*, September 1999, pp. 33-38.

[3] P. N. Favennec, H. L'Haridon, M. Salvi, D. Moutonnet, and Y. Le Guillou, *Electronic Letters 25,* 1989, p. 718.

[4] M. Dejneka and B. Samson, "Rare-Earth-Doped Fibers for Telecommunications Applications," *MRS Bulletin*, September 1999, pp. 39-45.

[5] A. J. Steckl, J. Heikenfeld, M. Garter, R. Birkhahn, D. S. Lee, "Rare Earth Doped Gallium Nitride—Light Emission from Ultraviolet to Infrared," *Compound Semiconductor,* 6(1), January/February 2000, pp. 48-52.

[6] A. J. Steckl and R. Birkhahn, "Visible Emission from Er-doped GaN Grown by Solid Source Molecular Beam Epitaxy," Applied Physics Letters, vol. 73, no. 12, pp. 1700-1702, 1998.

[7] A. Taguchi and K. Takahei, "Erbium in Si: Estimation of energy transfer rate and trap depth temperature dependence of intra-4f-shell luminescence," *Journal of Applied Physics*, vol 83, p. 2800, 1998.

[8] S. Campbell, *The Science and Engineering of Microelectronic Fabrication,* New York, Oxford University Press, 1996.

[9] P. D. Brown, "TEM Assessment of GaN epitaxial growth," Journal of Crystal Growth, vol 210, no. 1-3, March 2000, pp. 143-50.

[10] R. H. Birkhahn, R. Hudgins, D. S. Lee, B. K. Lee and A. J. Steckl, A. Saleh, R. G. Wilson, J. M. Zavada, "Optical and Structural Properties of Er-doped GaN Grown by MBE," *MRS Internet J. Nitride Semicond. Res.* 4S1, G3.80(1999).

[11] Desmond Lim, *Device Integration for Silicon Microphotonic Platforms,* PhD Thesis, MIT, 2000.

[12] H. Liu, Z. Ye, H. Zhang, B. Zhao, "Wurtzite GaN epitaxial growth on Si(111) using silicon nitride as an initial layer," *Materials Research Bulletin*, 35, pp. 1837-42, 2000.

[13] E. Hecht, *Optics,* New York, Addison Wesley Longman, Inc., 1998.

[14] B. E. A. Saleh, M. C. Teich, *Fundamentals of Photonics*, New York, John Wiley and Sons, 1991.

[15] E. M. Purcell, *Phys. Rev.* 211, 201, 1992.

[16] O. Madelung (Editor), *Semiconductors-Basic Data,* Berlin, Springer-Verlag, 1996.

[17] K. K. Lee, D. R. Lim, H.-C. Luan, A. Agarwal, J. Foresi, L. C. Kimerling, "Effect of size and roughness on light transmission in a Si/SiO2 waveguide: Experiments and model," Applied Physics Letters, vol. 77, no. 11, pp. 1617-9, 2000.

[18] F. P. Payne, J. P. R. Lacey, "A theoretical analysis of scattering loss from planar optical waveguides," *Optical and Quantum Electronics*, 26, 1994, pp.977-986.